



EMORY
LIBRARIES &
INFORMATION
TECHNOLOGY

OpenEmory

Experimental and Imaging Techniques for Examining Fibrin Clot Structures in Normal and Diseased States

Natalie K. Fan, *Georgia Institute of Technology*
Philip M. Keegan, *Georgia Institute of Technology*
[Manu Platt](#), *Emory University*
Rodney D. Averett, *Georgia Institute of Technology*

Journal Title: Journal of Visualized Experiments

Volume: Volume 2015, Number 98

Publisher: Journal of Visualized Experiments (JoVE) | 2015-04-01, Pages e52019-e52019

Type of Work: Article | Final Publisher PDF

Publisher DOI: 10.3791/52019

Permanent URL: <https://pid.emory.edu/ark:/25593/rxn6d>

Final published version: <http://dx.doi.org/10.3791/52019>

Copyright information:

© 2015 Journal of Visualized Experiments

Accessed January 22, 2020 9:27 AM EST

Video Article

Experimental and Imaging Techniques for Examining Fibrin Clot Structures in Normal and Diseased States

Natalie K. Fan¹, Philip M. Keegan¹, Manu O. Platt^{1,2}, Rodney D. Averett^{2,3}¹Wallace H. Coulter Department of Biomedical Engineering, Georgia Institute of Technology & Emory University School of Medicine²Parker H. Petit Institute for Bioengineering & Bioscience, Georgia Institute of Technology³George W. Woodruff School of Mechanical Engineering, Georgia Institute of TechnologyCorrespondence to: Rodney D. Averett at rdaverett@gatech.eduURL: <http://www.jove.com/video/52019>DOI: [doi:10.3791/52019](https://doi.org/10.3791/52019)

Keywords: Medicine, Issue 98, fibrin, clot, disease, confocal microscopy, diabetes, glycation, erythrocyte, sickle cell

Date Published: 4/1/2015

Citation: Fan, N.K., Keegan, P.M., Platt, M.O., Averett, R.D. Experimental and Imaging Techniques for Examining Fibrin Clot Structures in Normal and Diseased States. *J. Vis. Exp.* (98), e52019, doi:10.3791/52019 (2015).

Abstract

Fibrin is an extracellular matrix protein that is responsible for maintaining the structural integrity of blood clots. Much research has been done on fibrin in the past years to include the investigation of synthesis, structure-function, and lysis of clots. However, there is still much unknown about the morphological and structural features of clots that ensue from patients with disease. In this research study, experimental techniques are presented that allow for the examination of morphological differences of abnormal clot structures due to diseased states such as diabetes and sickle cell anemia. Our study focuses on the preparation and evaluation of fibrin clots in order to assess morphological differences using various experimental assays and confocal microscopy. In addition, a method is also described that allows for continuous, real-time calculation of lysis rates in fibrin clots. The techniques described herein are important for researchers and clinicians seeking to elucidate comorbid thrombotic pathologies such as myocardial infarctions, ischemic heart disease, and strokes in patients with diabetes or sickle cell disease.

Video Link

The video component of this article can be found at <http://www.jove.com/video/52019/>

Introduction

Injury to a blood vessel's endothelial lining is repaired through the hemostatic response, or the formation of a blood clot. When blood permeates into the extracellular matrix, tissue factors activate platelets in the blood stream that facilitate initiation of the coagulation cascade. The key mechanical component of this healing process is the fibrin matrix, composed of fibrin fibers that are highly elastic, and can sustain large forces¹⁻⁴. Many researchers have studied the formation structure, and function of fibrin extensively in the past decades⁵⁻¹³.

Patients with diseases such as diabetes mellitus and sickle cell have an increased risk of developing thrombotic complications such as myocardial infarctions, ischemic heart disease, and strokes¹⁴⁻¹⁹. Over 2 million people are newly diagnosed with diabetes mellitus each year in the United States. There are two types of diabetes: Type I, where the body fails to produce adequate amounts of insulin, and Type II, where the body becomes resistant to insulin. Among diabetic patients, cardiovascular disease (CVD) is the cause for 80% of the morbidity and mortality associated with the disease^{20,21}.

Sickle cell disease (SCD) is a genetic blood disorder that affects more than 100,000 people in the United States²². SCD is a point-mutation disease that causes red blood cells to become crescent-shaped, making it difficult for the cells to pass through the blood vasculature²³. Both of these disease states increase the chances of developing atherothrombotic conditions in the body. One of the reasons for this is a result of altered fibrin structure and function in diseased states^{14,24-26}.

In both diabetes and sickle cell disease, there is hypercoagulation and hypofibrinolysis activity that induces atherothrombosis and cardiovascular disease (CVD) as compared to healthy patients^{17,27,28}. It is known that hypofibrinolysis promotes atherosclerosis progression and engenders recurrent ischemic events for patients with premature coronary artery disease²⁹. In the current manuscript, we investigated the role of fibrin physical properties in this particular setting. Fibrin clot structures in non-diseased patients are composed of thin fibers, larger pores, and generally less dense^{14,24}. The increased porosity and less dense fibrin clots in healthy patients have been found to facilitate fibrinolysis¹⁶. In hyperthrombotic conditions such as diabetic and sickle cell disease, there is an increase in fibrinogen production, causing the fibrinogen concentration to increase from normal levels of 2.5 mg/ml in healthy patients³⁰⁻³³. Fibrin clots formed in diabetic patients have been found to be less porous, more rigid, have more branch points, and denser when compared to healthy, non-diabetic patients^{14,24,33-35}. The altered fibrin structure is a result of glycation mechanisms that occur in the proteins involved in clot formation. Nonenzymatic (irreversible) glycation occurs when glucose molecules bind to lysine residues on the fibrinogen molecule, which inhibits human factor XIIIa (FXIIIa) from properly cross-linking glutamine and lysine residues^{33,36,37}.

The structural analysis of fibrin networks has been studied extensively recently. In particular, researchers have utilized electron microscopy and 3D reconstruction of fibrin networks³⁸, investigated how both intravascular (endothelial) cells and extravascular (fibroblasts and smooth muscle) cells affect fibrin structure³⁹, utilized viscoelastic and spectral analysis to analyze fibrin structures⁴⁰, and developed correlations between fibrin structure and mechanical properties using experimental and computational approaches⁴¹. The focus of the current study was to formulate clot structures under simulated diabetic and sickle cell thrombosis conditions and to use confocal microscopy for examination of the structure and function of the clots in diseased states. Fibrin clots were formed from human fibrinogen, human thrombin, and FXIIIa. The clots were lysed using plasmin. To simulate diabetic conditions, increased concentration of fibrinogen was incubated in glucose solution to induce *in vitro* fibrinogen glycation. To simulate sickle cell disease clotting conditions, increased fibrinogen concentrations were mixed with sickle cell hematocrit collected from patients as done previously by our group⁴². These methods were used to examine the structure and functions involved in fibrin clot formation and fibrinolysis under diseased conditions, as well as the mechanisms that induce CVD. Based on current information about these diseases, the glycated fibrin clot structures were denser with fewer and smaller pores. The fibrin clots with red blood cells from sickle cell patients (RBCs) were also denser and displayed aggregation of the RBCs and agglomerated fibrin clusters. This is a well-established phenomenon that has been determined previously⁴³. It was also hypothesized that the fibrinolysis rate would be significantly lower in glycated fibrin clots with and without reduced plasmin compared to healthy, normal fibrin. The results showed that for glycated fibrin clots, significantly different lysis rate results were observed only under conditions of reduced plasmin concentration. This experimental technique of using confocal microscopy offers significant advantages over other imaging methods because the cells and proteins remain in their native state, which enables the capturing of real-time video of the clotting activity. This method of synthetically inducing clotting is also cheaper and more time efficient than obtaining patient samples and filtering out individual proteins and enzymes. Furthermore, by using separated proteins and enzymes to synthesize clots, the clots were standardized so that there was not variability between samples as a result of other proteins in the plasma.

Protocol

NOTE: The following protocol adheres to the guidelines set by the Institutional Review Board (IRB) at Georgia Tech.

1. Blood Collection and Red Blood Cell Isolation Procedure

1. Collect 40-120 ml of blood from donors in 10 ml heparinized vacutainer tubes. Start PBMC (peripheral blood mononucleated cell) isolation within 4 hr of collection. During this time, keep blood at RT.
NOTE: O/N storage of blood in RT or in 4 °C is **NOT** recommended as this will result in lower PBMC yield.
2. Dilute whole blood 1:1 in ice-cold (4 °C) sterile PBS.
3. Pipette 10 ml of ice-cold hydrophilic polysaccharide into an empty, sterile 50 ml conical tube. Gently transfer diluted whole blood on top of the hydrophilic polysaccharide.
4. Use a 25 ml pipette in slow setting and pipette blood along the side of the tube very slowly. Ensure that the blood is not mixed with the saccharide prior to centrifugation because the hydrophilic polysaccharide is toxic to cells and otherwise, the PBMC yield will be lower.
5. Centrifuge blood samples for 30 min at 400 x g at 4 °C. If available, reduce the brake speed of the centrifuge to half of maximum for better separation after centrifugation.
6. Aspirate off the plasma/platelet fraction of the centrifuged blood sample. Carefully aspirate off the hydrophilic polysaccharide layer directly above the packed RBC layer.
7. Collect 8-10 ml of packed RBCs and dilute 1:1 with unsterile 0.9% NaCl saline.

2. Confocal Microscopy Evaluation of Glycated Clot Structures (Simulated Diabetic Clots)

1. Defrost human fibrinogen and fluorescently labeled human fibrinogen conjugate at 37 °C.
2. Pipette the following into a 0.5 ml graduated microcentrifuge tube.
 1. For the healthy, normal fibrinogen clots, mix human fibrinogen with 10% fluorescently labeled human fibrinogen conjugate in a 50 mM Tris/100 mM NaCl buffer at a concentration of 5 mg/ml.
 2. For artificially glycated fibrinogen (to simulate diabetic clots), incubate human fibrinogen and 10% fluorescently labeled fibrinogen conjugate in a 5 mM solution of glucose dissolved in 50 mM Tris/100 mM NaCl for a resulting concentration of 6.8 mg/ml.
3. Cover the micro-centrifuge tubes using an opaque material to avoid exposure to light. Incubate the tubes in a 37 °C water bath for 48 hr.
4. Make a chamber on a glass microscope slide by affixing a thin adhesive on 2 sides of the slide.
5. After the 48 hr incubation period, prepare reagents for fibrin formation by defrosting FXIIIa and human alpha thrombin at RT.
6. Dilute FXIIIa to 80 U/ml in 5 mM CaCl₂ buffer.
7. Dilute thrombin to 4 U/ml in 5 mM CaCl₂ buffer.
 1. For normal clots, ensure that the final concentrations of fibrinogen, FXIIIa, and thrombin are 2.5 mg/ml, 20 U/ml, and 1 U/ml, respectively at a volume of 50 µl.
 2. For the glycated clots, ensure that the final concentrations of fibrinogen, FXIIIa, and thrombin are 3.4 mg/ml, 20 U/ml, and 1 U/ml, respectively at a volume of 50 µl.
8. Immediately pipette 30 µl of the fibrin solution into the chamber formed by the adhesive.
9. Place a 22 mm x 22 mm glass cover slip with thickness of 0.15 mm on top of the 2 layers of adhesive. Seal the open sides with clear adhesive to prevent the fibrin clot from drying out. Ensure that the adhesive does not interact with the fibrin clot.
10. Allow the fibrin clots to polymerize at 21-23 °C for 2 hr before confocal imaging.
11. Take confocal microscopy images of the clots using a confocal microscope with a 40X/1.30 Oil M27 lens with a 488 nm Argon laser.

3. Confocal Microscopy Evaluation of Fibrin Clots Containing RBCs from Sickle Cell Patients

1. Defrost human fibrinogen and fluorescently labeled human fibrinogen conjugate at 37 °C.
2. Pipette the following into a 0.5 ml graduated microcentrifuge tube.
 1. For the healthy, normal fibrin clot, mix human fibrinogen with 10% fluorescently labeled human fibrinogen conjugate in a 50 mM Tris/100 mM NaCl buffer at a concentration of 5 mg/ml.
 2. For the clots containing SCD RBCs, mix human fibrinogen and 10% fluorescently labeled human fibrinogen conjugate in a 50 mM Tris/100 mM NaCl such that the resulting concentration of the fibrinogen is 10 mg/ml.
3. Label the isolated RBCs (both normal and those from sickle cell patients obtained from the RBC isolation protocol) using a cell-labeling solution.
 1. Suspend cells at a density of 1×10^6 per ml in any chosen serum-free culture medium.
 2. Add 5 μ l/ml of the cell suspension to the cell-labeling solution. Mix well by gentle pipetting gently.
 3. Incubate for 20 min at 37 °C.
 4. Centrifuge the labeled suspension tubes at 1,500 rpm for 5 min at 37 °C.
 5. Remove the supernatant and gently re-suspend the cells in 37 °C medium.
 6. Repeat the wash procedure (3.3.4 and 3.3.5) two more times.
4. Dilute FXIIIa to 80 U/ml in 5 mM CaCl₂ buffer.
5. Dilute thrombin to 4 U/ml in 5 mM CaCl₂ buffer.
 1. For normal clots, ensure that the final concentrations of fibrinogen, FXIIIa, and thrombin are 2.5 mg/ml, 20 U/ml, and 1 U/ml, respectively at a volume of 50 μ l.
 2. For the clots containing SCD RBCs, ensure that the final concentrations of fibrinogen, FXIIIa, and thrombin are 5 mg/ml, 20 U/ml, and 1 U/ml, respectively at a volume of 50 μ l.
6. Pipette 10 μ l of the labeled RBCs into the fibrin solution. Pipette 30 μ l of the fibrin with RBCs onto the microscope glass (refer to slide preparation for glycated clots).
7. Allow the fibrin to polymerize at 21-23 °C for 2 hr before confocal imaging.
8. Take confocal images of the clots using the confocal microscope, and utilize excitation lasers with wavelengths of 488 nm and 633 nm to excite the fluorescently labeled fibrin and RBCs.

4. Confocal Microscopy Evaluation of Fibrinolysis Rates in Glycated Clot Structures

1. Repeat the confocal microscopy protocol of glycated clots (Protocol Step 2) for the fibrinolysis rate evaluation in glycated clots.
2. Do not seal the ends of the chamber with clear adhesive. Allow the fibrin clots to polymerize for 1.5 hr at 21-23 °C in a sealed enclosure containing 250 ml of water to prevent dehydration.
3. After polymerization, obtain images of the clots using the confocal microscope.
4. Pipette plasmin into the open end of the chamber and disperse the plasmin through the clot via capillary action.
 1. For the normal and glycated fibrinolysis experiments with normal concentrations, pipette 25 μ l at 200 μ g/ml of plasmin into the opening of the chamber.
 2. For the glycated clots with reduced concentrations, pipette 25 μ l at 50 μ g/ml into the opening of the chamber.
5. Use the time series feature (see **Figure 1**) in the confocal microscope software to capture real-time video footage of the plasmin lysing the clot.
 1. Click acquisition mode and then select "Time Series." Select the number of cycles and the recording time interval.

5. Calculating Fibrinolysis Rates

1. Determine the lysis rate by setting an area (2,500 μ m²) and calculating the elapsed time required to dissolve a fixed area of the clot. Calculate the lysis rate using the following equation (**Figure 2**):

$$\text{Plasmin lysis rate} = \frac{\text{clot area}}{\text{time to lyse the clot area}}$$

6. Statistical Analysis of Fibrinolysis Rates

1. Analyze the lysis data using statistical analysis software. Perform a one-way ANOVA and a *post hoc* Tukey-Kramer test^{44,45}.

Representative Results

Confocal Microscopy Analysis of Glycated Fibrin Clot Structures

The confocal microscopy images of normal and glycated clots are presented in **Figure 3**. Confocal microscopy analysis of the normal and glycated clots reveals that glycated clots are denser with smaller pores than the normal clots both with and without the addition of FXIIIa during

clot polymerization. In **Figure 3A** and **3B**, there is a lower fibrin concentration which created a less dense structure than the glycosylated clots with higher fibrin concentration (**Figures 3C** and **3D**).

The greater density observed (number of fibers per unit area) in the glycosylated clots is a result of the increased fibrinogen concentration that occurs in people with diabetes. In the normal clots, the fibrin fibers were more linear and formed longer fibers upon polymerization with FXIIIa, which is likely a result of the FXIIIa forming cross-links between the fibers. In the case of the glycosylated clots, the fibers appeared to be shorter, even with addition of FXIIIa. This is likely the result of the polymerization process that was altered due to the presence of glycosylated regions on the fibrinogen molecule. In addition, from analyzing **Figure 3**, it is likely that the fiber thickness was also reduced as a result of glycation, which is likely why the fluorescence from the glycosylated fibers appear to have a lower intensity.

Confocal Microscopy Analysis of Fibrin Clots Containing RBCs from Sickle Cell Patients

The confocal microscope images of the fibrin clot structure of clots with normal and RBCs from sickle cell patients are presented in **Figure 4**. As predicted, the confocal images of the fibrin clots containing RBCs from sickle cell patients had denser structures than those of healthy fibrin clots. **Figure 4A** shows a homogenous distribution of fibrin and normal RBCs. However, in **Figure 4B** there are clumps of fibrin and voids where no fibrin network formed. The RBCs from sickle cell patients were not homogeneously dispersed, but rather were embedded in the fibrin clumps. The increased density (number of fibers per unit area) was a result of the increased fibrinogen concentration that occurs as a result of hypercoagulation in SCD patients. Furthermore, the natural tendency of the RBCs from sickle cell patients to form aggregates engendered clumps of RBCs that became interwoven into the fibrin network. This resulted in the formation of aberrant clot structures that are markedly different in morphology than those in normal patients. From **Figure 4B**, it is observed that RBCs from sickle cell patients caused greater heterogeneity in the fibrin sample and also caused a wider spatial distribution of RBCs in the fibrin sample, when compared to the healthy fibrin clots with normal RBCs. In contrast, the healthy fibrin clots with normal RBCs displayed a more homogenous dispersion of cells throughout the fibrin network.

It is unknown how much HbS (sickle hemoglobin) was polymerized in the erythrocytes from sickle cell patients and is contained in the samples. What is known, however, is that the presence of any amount of HbS causes greater aggregation of cells in number of HbS molecules per unit volume vs. normal HbA molecules. Pan *et al.*⁴⁶ have demonstrated this phenomenon in a study where they compared the aggregation/clustering effects of deoxy-HbS, and, for comparison, of oxy-HbS and oxy-normal adult hemoglobin, HbA. The clusters formed within a few seconds after solution preparation and their sizes and numbers remained relatively steady for up to 3 hr. One of the conclusions from the study was that both oxy-HbS and deoxy-HbS molecules clustered at a higher number density than oxy-HbA (normal) molecules as a function of temperature. Pertaining to the current study, this means that the RBCs from sickle cell patients were likely to cluster together, and trapped fibrin as it was being polymerized from the fibrinogen precursor.

Confocal Microscopy Lysis Rate Analysis of Normal and Glycosylated Clots

It was hypothesized that the fibrinolysis rates would be greater for normal fibrin clots compared to glycosylated fibrin clots with decreased plasmin concentration. To test this hypothesis, confocal microscopy was used to assess the lysis rates of fibrin clots with the addition of plasmin. The average (mean) lysis rates of normal fibrin with the addition of 200 $\mu\text{g/ml}$ of plasmin was $43.2 \pm 26.5 \mu\text{m}^2/\text{sec}$ and the average (mean) lysis rates of glycosylated fibrin with the addition of 200 $\mu\text{g/ml}$ of plasmin was $29.7 \pm 11.2 \mu\text{m}^2/\text{sec}$. For the glycosylated fibrin clot lysed with 50 $\mu\text{g/ml}$ of plasmin, the average lysis rate was $12.8 \pm 3.1 \mu\text{m}^2/\text{se}$. A total of 10 samples each (30 samples) were used to determine the average and standard deviation values. These values are presented in **Figure 5**. A p-value of 0.05 was used to determine significance between the independent experimental groups. Analysis of the fibrinolysis rates demonstrated that the value for the normal clots compared to the glycosylated (simulated diabetic) clots with decreased plasmin were significantly different.

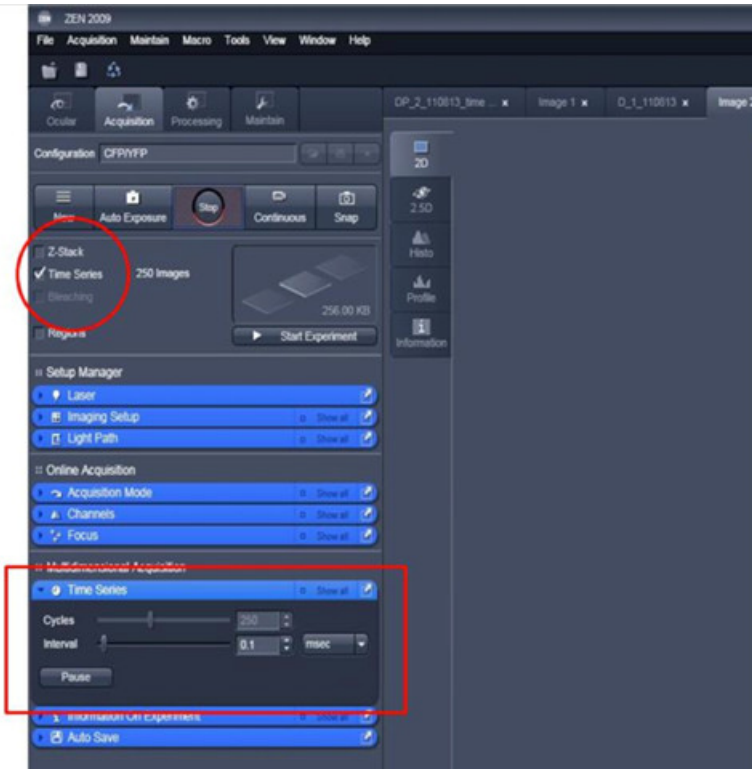


Figure 1. Sample screenshot from confocal microscope software detailing method for obtaining real-time, continuous imaging of fibrin clot lysis. [Please click here to view a larger version of this figure.](#)

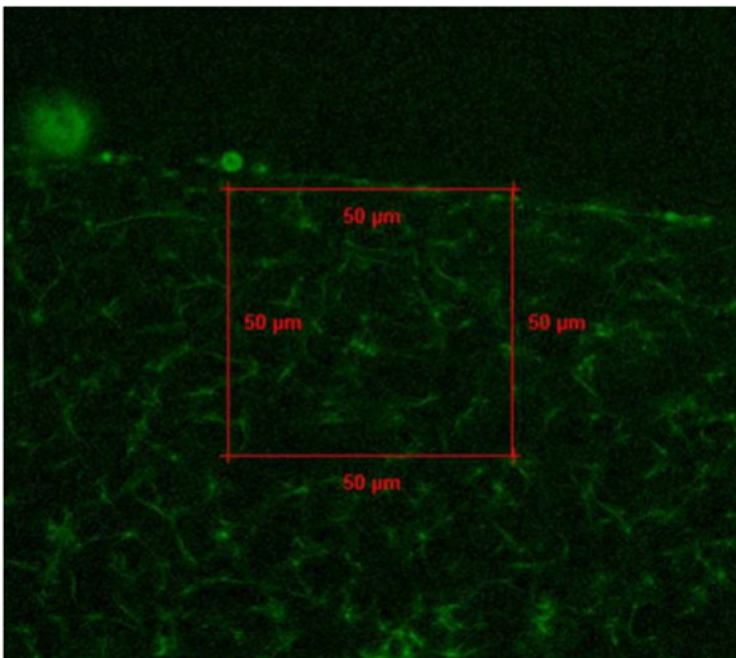


Figure 2. Example confocal image with fixed area used to calculate lysis rate of fibrin clot sample. [Please click here to view a larger version of this figure.](#)

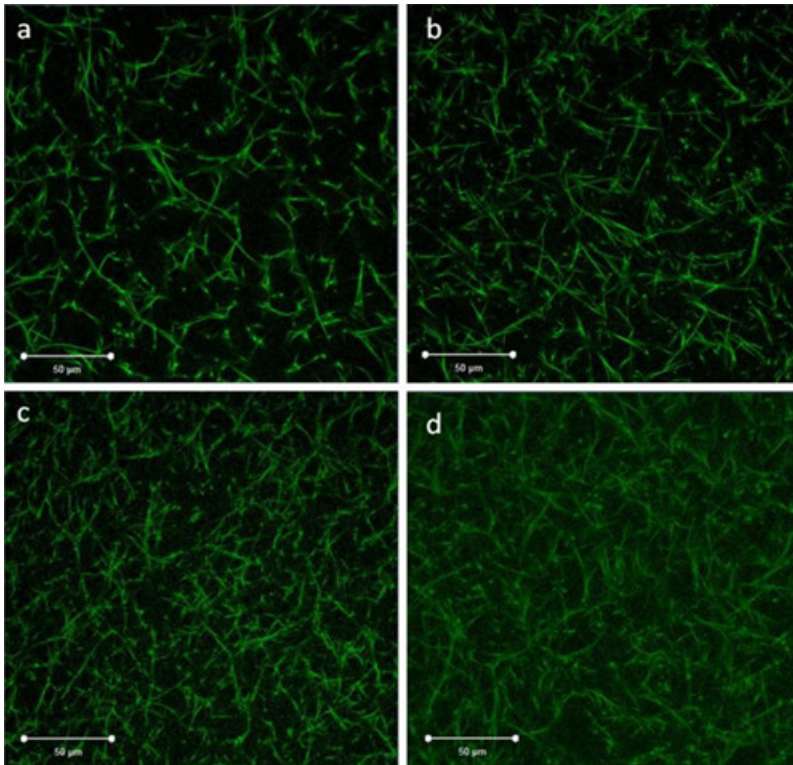


Figure 3. Confocal images of healthy and glycosylated (diabetic) fibrin clots. Green fluorescence represents the fibrin network. The unglycosylated fibrin represents clots formed in healthy patients, whereas glycosylated fibrin represents clots formed in diabetic patients. (A) Unglycosylated fibrin without the addition of FXIIIa. (B) Unglycosylated fibrin with FXIIIa. (C) Glycosylated fibrin without FXIIIa and (D) Glycosylated fibrin with FXIIIa. The red scale bar indicates 50 µm. [Please click here to view a larger version of this figure.](#)

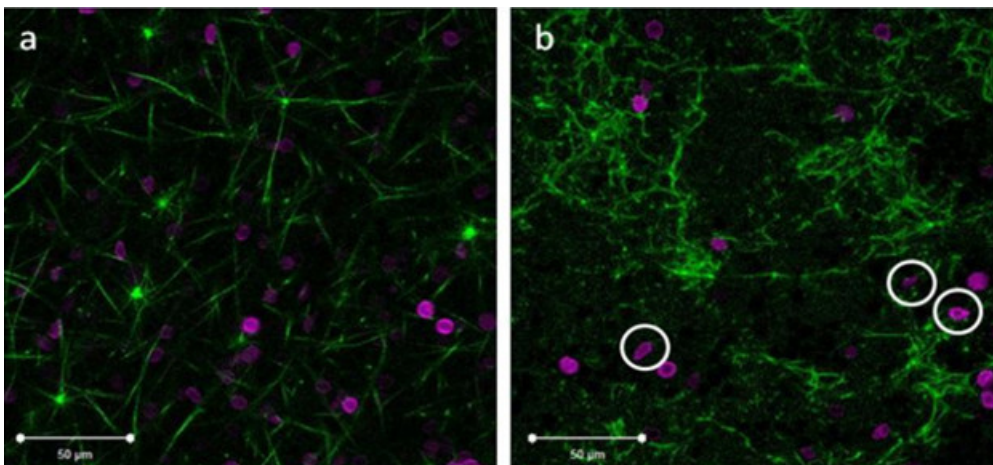


Figure 4. Confocal images of healthy fibrin clots with normal RBCs and fibrin clots with RBCs from sickle cell patients. Green fluorescence represents the fibrin network and magenta represents labeled healthy and RBCs from sickle cell patients. (A) Healthy RBCs in normal fibrin concentration with FXIIIa and (B) Increased fibrin with FXIIIa and RBCs from a sickle cell patient. The white scale bar indicates 50 µm. The white circles in image (B) indicate recognizable sickled RBCs. [Please click here to view a larger version of this figure.](#)

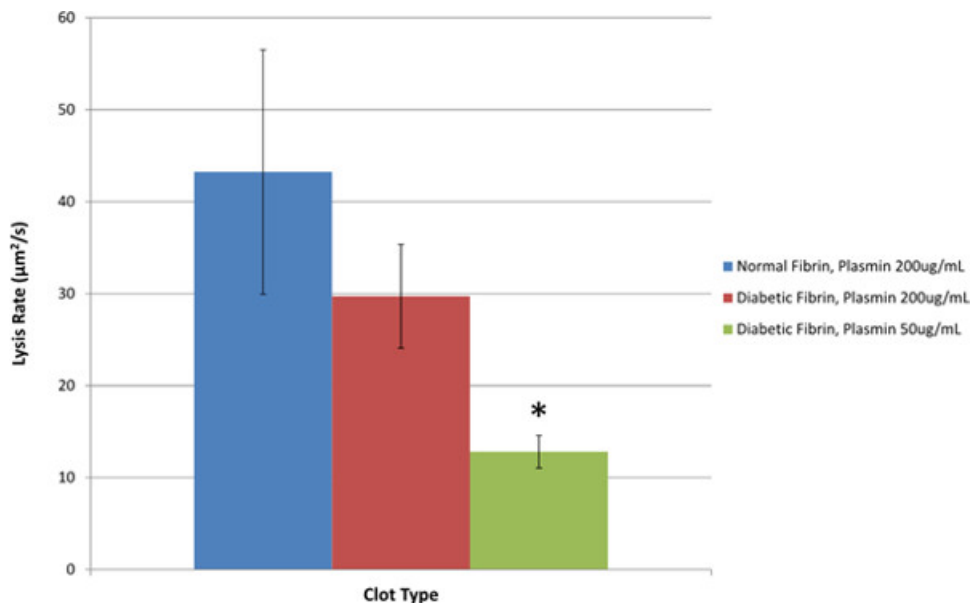


Figure 5. Fibrinolysis rates of normal fibrin clots compared to glycosylated (diabetic) fibrin clots and glycosylated clots with reduced plasmin concentration. Statistical significance was determined based on a one-way ANOVA and a *post hoc* Tukey-Kramer multiple comparison test. The ANOVA analysis showed that there was a significant difference between lysis rate means. The Tukey-Kramer test showed that there was a significant difference in means between the normal clots and clots with decreased plasmin with a $p < 0.05$. The * indicates a significant difference from normal clots.

Discussion

To obtain meaningful data about the structure of clotting mechanisms in disease states, it is important to isolate the factors involved in clotting to determine the effects of the proteins and cells in these conditions. This protocol was developed for the purposes of investigating the structure of the fibrin clot in diabetic and SCD states *in vitro*.

It is necessary to understand the mechanisms involved in fibrin formation and fibrinolysis in disease states since altered conditions cause hypercoagulation, atherothrombosis, and CVD. From the confocal images obtained in this experiment, it is evident that hypercoagulation activity occurs in diabetic and SCD states, which causes an increased fibrinogen concentration. An increased fibrinogen concentration results in a denser fibrin network with more branch points and smaller pores throughout the network. In fibrin networks of SCD patients, not only is there more fibrin present, but the aggregating nature of the erythrocytes from sickle cell patients also changes the structure of the network as it entraps fibrin into clusters. The conglomeration of RBCs from sickle cell patients also reduces porosity of the fibrin clusters in the network, but appears to increase void concentration in the overall network. The results of the fibrinolysis analysis of the glycosylated clots supported the hypothesis of the lysis rate in glycosylated clots being lower with reduced plasmin than that of healthy, normal clots. However, the results did not provide conclusive evidence about lysis rates of glycosylated clots with normal concentrations of plasmin. Thus it can be concluded that for diabetic patients with normal plasmin concentration, there may be sufficient fibrinolysis activity to degrade fibrin clots in an efficient manner.

For the experiments performed in this research study, isolated proteins and RBCs were used, instead of whole blood and plasma. By using separated proteins to synthesize the fibrin clots, the causes for altered structures between the normal vs. diseased clots could be determined. This greatly reduced the possibility of having other plasma proteins interfere with the structure and morphology of the fibrin clots. However, by using isolated proteins, it is crucial to store and handle the cells and proteins properly, as they are more vulnerable to cell death and protein degradation.

The confocal microscopy imaging technique chosen for this study was due to the ability to obtain images of the fibrin clot structures while retaining the natural thrombotic properties of the cells and proteins. Confocal microscopy has also been shown to give improved contrast and optical resolution of the specimen with reduced noise compared to traditional light microscopy. The laser light is directed into a pinhole that blocks unfocused light from entering. Utilization of confocal microscopy obviated the need for the addition of fixative chemicals; thus the cells and proteins were able to maintain their natural protein activity of forming fibrin clots. As a result the cells, proteins, and enzymes functioned in their native state, allowing the use of confocal microscopy for capturing images and video of real-time activity. With confocal microscopy, 3D images of the fibrin clots were captured and videos of plasmin digestion of fibrin clots were obtained in real-time. When adding plasmin to the clot to capture a time series video of the clot lysis process, it was important to use capillary action via plasmin to homogeneously disperse the enzyme through the fibrin matrix. This was done to ensure that the added plasmin concentration was accurate and allowed the enzyme to lyse the entire clot, in contrast to the local area that the plasmin was added.

The method and the results obtained in this study were similar to a study done by Dunn *et al.*, who found that clot lysis rates were significantly lower in diabetic subjects than control subjects²⁵. In both studies, there were significant differences in lysis rates of diabetic (glycosylated) clots; however, the current protocol may accurately represent diabetic states because of the reduced plasmin levels. Additionally, in this research study fibrinolysis was captured continuously in real-time using the confocal microscope, in contrast to analyzing discrete sections at different time intervals. Wootton *et al.*⁴⁷ have investigated fibrin clot lysis and employed a lysis front velocity (cm/s) to investigate the rate of lysis for clots. They used confocal image analysis in their study to determine the front velocity. In the current study, instead of a lysis front velocity, a lysis area

velocity was used (because of the way the image was analyzed on the confocal). To further validate the method developed in our study, the authors in ⁴⁸ have described a mathematical model of fibrin clot lysis by plasmin, in which they prescribe the lysis front velocity as a function of the effective rate constant of fibrinolysis. The equation is given as:

$$\frac{dX}{dt} = \frac{1}{\rho_{Fn}} \left(\frac{k_{eff} K_a C_{pm}}{1 + K_a C_{pm}} \right).$$

Here, $\frac{dX}{dt}$ represents the effective rate constant of fibrinolysis, K_a is the adsorption constant, C_{pm} is the plasmin concentration, and ρ_{Fn} is the density of fibrin. If the measured quantity $\frac{dA}{dt}$ (measured from the confocal analysis in the current study) is utilized and the chain rule is employed, this leads to:

$$\frac{dA}{dt} = x \frac{dy}{dt} + y \frac{dx}{dt}$$

Assuming only one dimension is changing per unit time leads to:

$$\frac{dA}{dt} = y \frac{dx}{dt}$$

$$\frac{1}{y} \frac{dA}{dt} = \frac{dx}{dt}$$

Thus the effective rate constant of fibrinolysis for the experiment leads to:

$$k_{eff} = \rho \frac{1}{y} \frac{dA}{dt} \left(\frac{1 + K_a C_{pm}}{K_a C_{pm}} \right)$$

This relationship infers that the effective rate constant of fibrinolysis ($k_{eff} \left[\frac{mg}{cm^2 \cdot min} \right]$) is a function of the plasmin concentration (C_{pm}) and the area lysis rate $\frac{dA}{dt}$.

This technique is also important for the study of thrombosis in SCD patients, since there is little known about fibrin and clotting mechanisms with respect to this disease. There have been very few studies conducted on the effects of SCD on the structure of fibrin clots; thus the confocal images collected from this study provides rare visualization of the clot structure with incorporated sickled RBCs.

To compare the differences in means between the groups, use a one-way ANOVA and a *post hoc* Tukey-Kramer test. A one-way ANOVA is a statistical test used to determine a statistically significant difference in the means between independent groups. The Tukey-Kramer post-test is used to compare the means from each independent group and determine which groups' means are statistically different from each other. Before performing a one-way ANOVA, there are six assumptions that must be met to ensure that the results are valid. The six assumptions are: a continuous dependent variable (lysis rate), an independent variable consisting of two or more independent categorical groups (normal, glycated, and glycated with reduced plasmin), and independently observed data in each group such that one event occurring does not affect another event (This assures that there is no overlap in data.), the dataset not containing any significant outliers, normally distributed data verified by the Shapiro-Wilk statistical test, and homogeneity of variances in the data verified by the Levene statistical test. Once these assumptions were met, a one-way ANOVA and a *post hoc* Tukey-Kramer test were performed with a p-value of 0.05 as the threshold for determining statistical significance. For a rigorous detail of the one-way ANOVA and post-hoc Tukey-Kramer test, refer to ^{44,45}.

Overall, this method allows for imaging of normal and abnormal (due to diseased states) fibrin clots in their native states. The method also provides details for real-time imaging of clot lysis as well as statistical analysis of lysis rates. The ease with which the thrombus can be produced and imaged *in vitro* is useful for a wide range of applications in cellular and tissue engineering.

Disclosures

The authors have nothing to disclose.

Acknowledgements

The authors would like to thank the Lam Lab at Georgia Tech for many helpful discussions in developing the experimental assays. Research reported in this publication was supported by the National Heart, Lung, and Blood Institute of the National Institutes of Health under Award Number K01HL115486 and by New Innovator Grant 1DP2OD007433-01 from the Office of the Director, National Institutes of Health. The content is solely the responsibility of the authors and does not necessarily represent the official views of the National Institutes of Health.

References

1. Averett, R. D., *et al.* A Modular Fibrinogen Model that Captures the Stress-Strain Behavior of Fibers. *Biophysical Journal*. **103**, 1537-1544 (2012).
2. Carlisle, C. R., *et al.* The mechanical properties of individual, electrospun fibrinogen fibers. *Biomaterials*. **30**, 1205-1213 (2009).
3. Falvo, M. R., Gorkun, O. V., Lord, S. T. The molecular origins of the mechanical properties of fibrin. *Biophysical Chemistry*. **152**, 15-20 (2010).
4. Guthold, M., Cho, S. S. Fibrinogen Unfolding Mechanisms Are Not Too Much of a Stretch. *Structure*. **19**, 1536-1538 (2011).
5. Gerth, C., Roberts, W. W., Ferry, J. D. Rheology of fibrin clots II: Linear viscoelastic behavior in shear creep. *Biophysical Chemistry*. **2**, (74), 208-217 (1974).
6. Nelb, G. W., Kamykowski, G. W., Ferry, J. D. Rheology of fibrin clots. v. shear modulus, creep, and creep recovery of fine unligated clots. *Biophysical Chemistry*. **13**, (81), 15-23 (1981).
7. Roberts, W. W., Kramer, O., Rosser, R. W., Nestler, F. H. M., Ferry, J. D. Rheology of fibrin clots. I.: Dynamic viscoelastic properties and fluid permeation. *Biophysical Chemistry*. **1**, 152-160 (1974).
8. Ryan, E. A., Mockros, L. F., Weisel, J. W., Lorand, L. Structural Origins of Fibrin Clot Rheology. *Biophysical Journal*. **77**, 2813-2826 (1999).
9. Weisel, J. W. Fibrin assembly. Lateral aggregation and the role of the two pairs of fibrinopeptides. *Biophysical Journal*. **50**, 1079-1093 (1986).
10. Weisel, J. W. The mechanical properties of fibrin for basic scientists and clinicians. *Biophysical Chemistry*. **112**, 267-276 (2004).
11. Wolberg, A. S. Thrombin generation and fibrin clot structure. *Blood Reviews*. **21**, 131-142 (2007).
12. Wolberg, A. S., Campbell, R. A. Thrombin generation, fibrin clot formation and hemostasis. *Transfusion and Apheresis Science*. **38**, 15-23 (2008).
13. Yeromonahos, C., Polack, B., Caton, F. Nanostructure of the Fibrin Clot. *Biophysical Journal*. **99**, 2018-2027 (2010).
14. Dunn, E. J. Fibrinogen and fibrin clot structure in diabetes. *Herz*. **29**, 470-479 (2004).
15. Gladwin, M. T., Sachdev, V. Cardiovascular abnormalities in sickle cell disease. *Journal of the American College of Cardiology*. **59**, 1123-1133 (2012).
16. Collet, J. P., *et al.* Altered Fibrin Architecture Is Associated With Hypofibrinolysis and Premature Coronary Atherothrombosis. *Arteriosclerosis, thrombosis, and vascular biology*. **26**, 2567-2573 (2006).
17. Carr, M. E. Diabetes mellitus: a hypercoagulable state. *Journal of Diabetes and its Complications*. **15**, 44-54 (2001).
18. Ajjan, R. A., Ariens, R. A. S. Cardiovascular disease and heritability of the prothrombotic state. *Blood Reviews*. **23**, 67-78 (2009).
19. Standeven, K. F., Ariens, R. A. S., Grant, P. J. The molecular physiology and pathology of fibrin structure/function. *Blood Reviews*. **19**, 275-288 (2005).
20. American Diabetes Association. Available from: <http://www.diabetes.org/> (2014).
21. Alzahrani, S., Ajjan, R. Review article: Coagulation and fibrinolysis in diabetes. *Diabetes and Vascular Disease Research*. **7**, 260-273 (2010).
22. Sickle Cell Disease Association of America, Inc. Available from: <http://www.sicklecelldisease.org/> (2014).
23. Stuart, M. J., Nagel, R. L. Sickle-cell disease. *The Lancet*. **364**, 1343-1360 (2004).
24. Dunn, E. J., Ariens, R. A. S., Grant, P. J. The influence of type 2 diabetes on fibrin structure and function. *Diabetologia*. **48**, 1198-1206 (2005).
25. Dunn, E. J., Philippou, H., Ariens, R. A. S., Grant, P. J. Molecular mechanisms involved in the resistance of fibrin to clot lysis by plasmin in subjects with type 2 diabetes mellitus. *Diabetologia*. **49**, 1071-1080 (2006).
26. Famodu, A., Reid, H. Plasma fibrinogen levels in sickle cell disease. *Tropical and geographical medicine*. **39**, 36-38 (1987).
27. Richardson, S., Matthews, K., Stuart, J., Geddes, A., Wilcox, R. Serial Changes in Coagulation and Viscosity during Sickle-Cell Crisis. *British journal of haematology*. **41**, 95-103 (1979).
28. Ataga, K. I., Orringer, E. P. Hypercoagulability in sickle cell disease: a curious paradox. *The American Journal of Medicine*. **115**, 721-728 (2003).
29. Collet, J. P., *et al.* Altered fibrin architecture is associated with hypofibrinolysis and premature coronary atherothrombosis. *Arteriosclerosis, thrombosis, and vascular biology*. **26**, 2567-2573 (2006).
30. Barazzoni, R., *et al.* Increased Fibrinogen Production in Type 2 Diabetic Patients without Detectable Vascular Complications: Correlation with Plasma Glucagon Concentrations. *The Journal of Clinical Endocrinology & Metabolism*. **85**, 3121-3125 (2000).
31. Ceriello, A. Coagulation activation in diabetes mellitus: the role of hyperglycaemia and therapeutic prospects. *Diabetologia*. **36**, 1119-1125 (1993).
32. Mayne, E. E., Bridges, J. M., Weaver, J. A. Platelet adhesiveness, plasma fibrinogen and factor VIII levels in diabetes mellitus. *Diabetologia*. **6**, 436-440 (1970).
33. Weisel, J. W. Fibrinogen and fibrin. *Advances in protein chemistry*. **70**, 247-299 (2005).
34. Collet, J., *et al.* Influence of Fibrin Network Conformation and Fibrin Fiber Diameter on Fibrinolysis Speed Dynamic and Structural Approaches by Confocal Microscopy. *Arteriosclerosis, thrombosis, and vascular biology*. **20**, 1354-1361 (2000).
35. Jörniskog, G., *et al.* Altered properties of the fibrin gel structure in patients with IDDM. *Diabetologia*. **39**, 1519-1523 (1996).
36. Svensson, J., *et al.* Acetylation and glycation of fibrinogen in vitro occur at specific lysine residues in a concentration dependent manner: A mass spectrometric and isotope labeling study. *Biochemical and Biophysical Research Communications*. **421**, 335-342 (2012).
37. Pieters, M., *et al.* Glycation of fibrinogen in uncontrolled diabetic patients and the effects of glycaemic control on fibrinogen glycation. *Thrombosis Research*. **120**, 439-446 (2007).
38. Baradet, T. C., Haselgrove, J. C., Weisel, J. W. Three-dimensional reconstruction of fibrin clot networks from stereoscopic intermediate voltage electron microscope images and analysis of branching. *Biophysical journal*. **68**, 1551-1560 (1995).
39. Campbell, R. A., Overmyer, K. A., Selzman, C. H., Sheridan, B. C., Wolberg, A. S. Contributions of extravascular and intravascular cells to fibrin network formation, structure, and stability. *Blood*. **114**, 4886-4896 (2009).
40. Curtis, D. J., *et al.* A study of microstructural templating in fibrin-thrombin gel networks by spectral and viscoelastic analysis. *Soft Matter*. **9**, 4883-4889 (2013).
41. Kim, E., *et al.* Correlation between fibrin network structure and mechanical properties: an experimental and computational analysis. *Soft Matter*. **7**, 4983-4992 (2011).
42. Keegan, P. M., Surapaneni, S., Platt, M. O. Sickle cell disease activates peripheral blood mononuclear cells to induce cathepsins k and v activity in endothelial cells. *Anemia*. **2012**, 201781 (2012).

43. Allison, A. Properties of sickle-cell haemoglobin. *Biochemical Journal*. **65**, 212 (1957).
44. Kuehl, R. O. *Design of experiments : statistical principles of research design and analysis*. Cengage Learning Pacific Grove, CA (2000).
45. Lindman, H. R. *Analysis of variance in experimental designs*. Springer-Verlag Publishing New York, N.Y., USA (1992).
46. Pan, W., Galkin, O., Filobelo, L., Nagel, R. L., Vekilov, P. G. Metastable Mesoscopic Clusters in Solutions of Sickle-Cell Hemoglobin. *Biophysical Journal*. **92**, 267-277 (2007).
47. Wootton, D. M., Popel, A. S., Alevriadou, B. R. An experimental and theoretical study on the dissolution of mural fibrin clots by tissue-type plasminogen activator. *Biotechnology and bioengineering*. **77**, 405-419 (2002).
48. Sazonova, I. Y., *et al.* 127 Mathematic model of fibrin clot lysis by plasmin. *Fibrinolysis and Proteolysis*. **12**, Suppl 1. 45 (1998).